Numerical Analysis and Comparison of Airflow in Rotors with U and V Groove during Rotor Spinning Process

Rui-Hua Yang, PhD, Chao Liu, Yuan Xue, Hongbo Wang, Weidong Gao

Key Laboratory of Eco-textiles, Jiangnan University, Wuxi, Jiangsu Province CHINA

Correspondence to:
Rui-Hua Yang email: yangrh@jiangnan.edu.cn

ABSTRACT

Rotor spinning is known for high production rates and uniformity of the resulting yarn. However, determining machine components which will produce the optimum process parameters such as airflow speed to result in the best combinations of yarn quality and uniformity can be a difficult task. The aim of this study is to simulate and analyze the airflow characteristics in rotors with U and V grooves during the rotor spinning process. The results obtained showed that airflow speed resulting from a rotor with the V groove is higher than that of U type. As a result, the static pressure resulting from the use of the V type groove is lower than that of U groove.

Keywords: Rotor spinning, groove, airflow, pressure, speed

INTRODUCTION

Rotor spun yarn is one of the most common coarse yarns in the textile market [1-5]. The key parts of rotor spinning consist of the rotor, feeding-combing mechanism, navel and yarn take up and delivery systems [6]. All components of the system are contained in a single box, called the 'spin box'. During the rotor spun yarn spinning process is fed into the feed plate, and then fibers are gathered on the collection groove of the rotor, inserting twist into the fibers. The yarn produced is then taken up onto a cross wound package, as illustrated by *Figure 1*, eliminating the need for a separate winding process, as in ring spinning. The type of groove in the rotors determines fiber type that can be used and yarn thickness that can be produced with a given system. U and V are most widely used types of rotor grooves (*Figure 2)* and both are adaptable to various fiber and yarn types. In this paper, the static pressure and air flow speeds produced by rotors (diameter 46 mm) with U and V grooves will be simulated and analyzed.

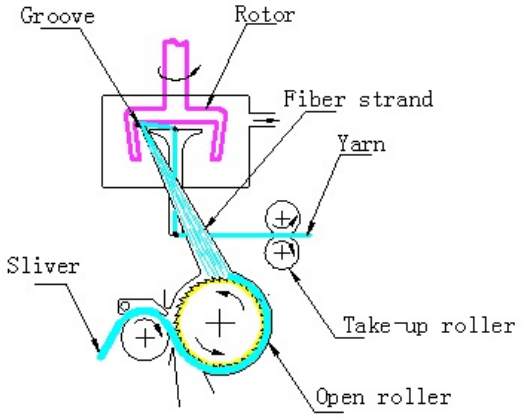

FIGURE 1. Rotor spun yarn spinning process.

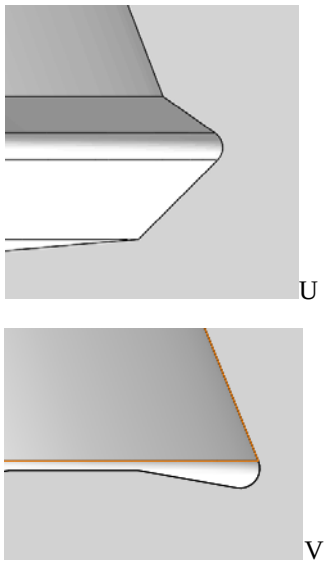

FIGURE 2. Geometric sketch of collection grooves.

MODELS

The airflow during rotor spinning process obeys mass conservation and momentum conservation based upon fluid mechanics [7-9].

Mass conservation according to Eq. (1):

$$\frac{\partial(\rho u_k)}{\partial x_k} = 0 \tag{1}$$

Where u_k is the air velocity in x_k direction and ρ is air density.

Momentum conservation according to Eq. (2):

$$\frac{\partial(\rho u_i u_k)}{\partial x_k} = -\frac{\partial p}{\partial x_i} + \frac{1}{\mathrm{Re}}\frac{\partial \tau_{ij}}{\partial x_j} \tag{2}$$

Where ρ is air density, u_k is the air velocity in the x_k direction, p is air pressure, Re is Reynolds number, and τ_{ij} is the tensor of Newton fluid viscous stress from Eq. (3):

$$\tau_{ij} = \mu\left(\frac{\partial u_i}{\partial x_j} + \frac{\partial u_j}{\partial x_i}\right) - \frac{2}{3}\mu\frac{\partial u_k}{\partial x_k}\delta_{ij} \tag{3}$$

Where μ is coefficient of dynamic viscosity, and δ_{ij} is the function of Komecker delta.

The standard k-ε turbulent model is applied to simulate the motion of air flow in rotor as in Eqs. (4) and (5):

$$\frac{\partial(\rho k)}{\partial t} + \frac{\partial(\rho k u_i)}{\partial x_i} = \frac{\partial}{\partial x_j}\left[\left(\mu + \frac{\mu_t}{\sigma_t}\right)\frac{\partial k}{\partial x_j}\right] + G_k + G_b - \rho\varepsilon - Y_M + S_k \tag{4}$$

$$\frac{\partial(\rho\varepsilon)}{\partial t} + \frac{\partial(\rho\varepsilon u_i)}{\partial x_i} = \frac{\partial}{\partial x_j}\left[\left(\mu + \frac{\mu_t}{\sigma_\varepsilon}\right)\frac{\partial \varepsilon}{\partial x_j}\right] + C_{1\varepsilon}\frac{\varepsilon}{k}\left(G_k + C_{3\varepsilon}G_b\right) - C_{2\varepsilon}\rho\frac{\varepsilon^2}{k} + S_\varepsilon \tag{5}$$

Where G_k is the result of turbulent kinetic energy k which is generated by the average velocity gradient, G_b is the result of turbulent kinetic energy b which is generated by buoyancy, Y_M is a result of pulsation expansion in the compressible turbulent flow, $C_{1\varepsilon}$、$C_{2\varepsilon}$ and $C_{3\varepsilon}$ are experimental constants, σ_k and σ_ε are Prandtl numbers according to turbulent energy k and dissipative energy ε separately. S_k and S_ε are source terms defined by users.

According to the recommended value by Launder et al. [10] and experimental verification, in this paper, model constants are determined as $C_{1\varepsilon}$=1.42，$C_{2\varepsilon}$=1.68，$C_{3\varepsilon}$=0.09，σ_k=1.0，σ_ε=1.3.

It is assumed that the airflow speed of inlet is 0.0054 m^3/s and the pressure of outlet is -8000Pa and the rotor speed is 120000r/min (Diameter 46 mm with U and V grooves respectively). The SIMPLE algorithm (Semi-Implicit Method for Pressure-Linked Equations) is used to solve the pressure and velocity coupled. The standard k-turbulent model is used to simulate air turbulence, since the wall function method is used here. No slip boundary conditions are used at the wall. A geometric model of the spin box is shown in *Figure 3*.

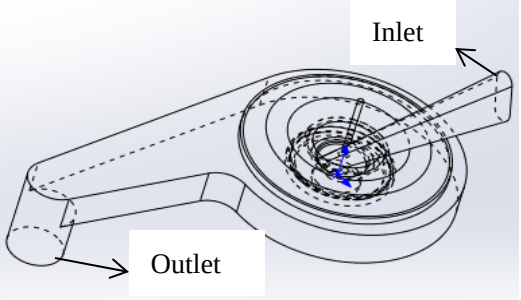

FIGURE 3. Geometric model of spin box.

RESULTS AND DISCUSSION

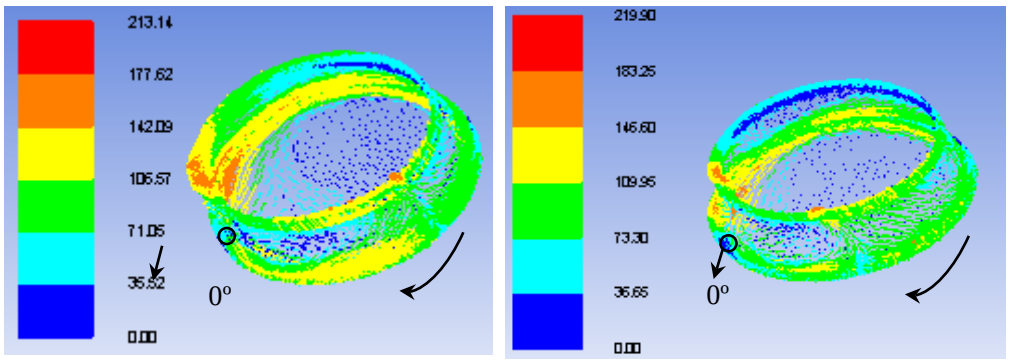

U V

FIGURE 4. Airflow speed of rotors (U-type and V-type).

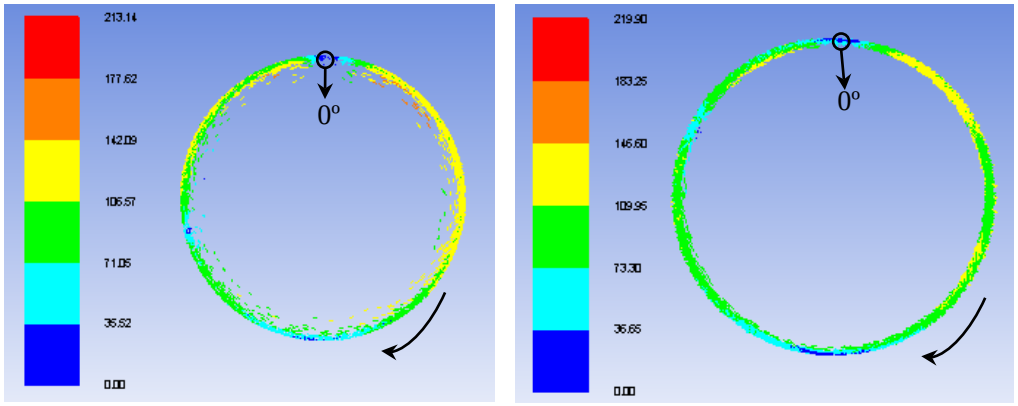

U V

FIGURE 5. Airflow speed of grooves (U-type and V-type).

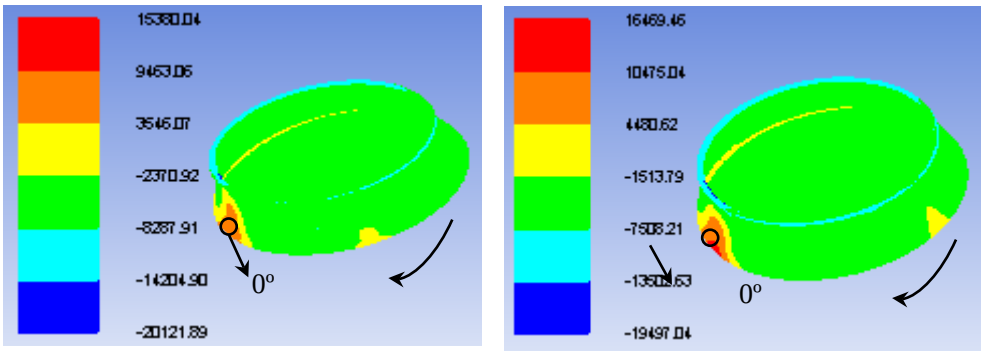

U V

FIGURE 6. Static pressure distribution of rotors (U-type and V-type).

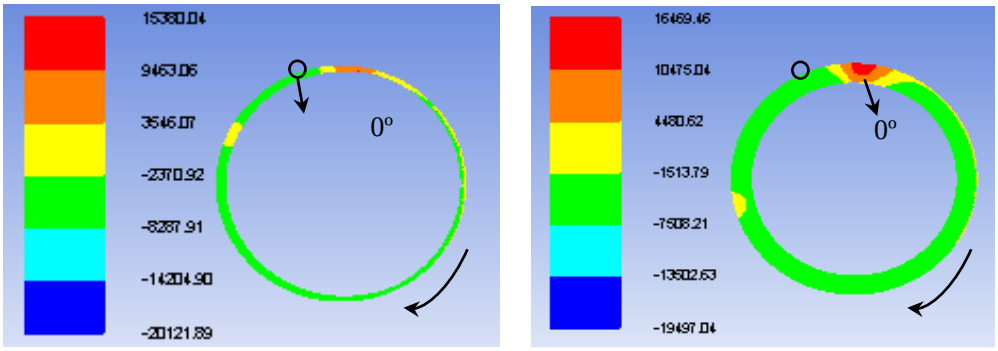

U V

FIGURE 7. Static pressure distribution of grooves (U-type and V-type).

Airflow speeds and pressures of rotors and grooves are illustrated by *Figures 4-7*. They show that airflow speed of the rotor and groove of the U-type (106-142m/s) is slower than that with V-type (109-146 m/s). As a result, the static pressures of rotor and groove of the U type are lower than that of V-type (-8287 Pa vs. -7508 Pa). It can also been seen that airflow speed and static pressure is not steady at the rotor or groove wall. To understand how the speed and pressure in the groove wall affect the spinning process, the pressure and speed of a single 0^o to 360^o rotation of the rotor groove are illustrated by *Figure 8* and *Figure 9*, respectively. It is assumed that 0^o is the cross point of fiber transport channel and groove, and angles increase in the clockwise rotation direction of the rotor.

Airflow speeds of U and V grooves at the groove wall show the same trend, in the shape of the letter 'M', as shown by *Figure 8*. It can be determined that air flow speed was lowest at 0^o, and then increased rapidly to 135m/s at 20^o rotation. From 20^o to 100^o, the speed is nearly stable, which is a favorable condition for the combination of fibers. The airflow speed then decreased sharply to 30 m/s at 180^o, before increasing again to 110 m/s at 280^o, and then becoming nearly stable until 340 degrees of rotation.

During the rotor spinning process, the fibers enter the incline wall, which is called the slip wall inside the rotor, as shown by *Figure 1*. Under the action of the centrifugal force of rotor rotation, the fibers slip into the groove, and are circulated and piled up into rings like laminated layers, called the 'fibrous ring' or 'yarn ring tail', which exerts a doubling effect. When the piecing yarn enters the rotor, it is thrown into the collecting groove and joined with the 'fibrous ring' [6]. Then the delivery rollers deliver the yarn from the machine and simultaneously the rotor rotation twists the yarn tail. Since the airflow speed reaches a minimum point at three separate rotation angles (0^o, 180^o and 360^o in *Figure 8*), the yarn ring tail must forming well before the fiber reached the angle of 360 degrees. This agrees with the experimental data, which shows that that yarn tail is combined with the piecing yarns and twisted during the region of 320^o - 340^o rotation, before it reaches the cross point of the fiber transport channel and groove (0^o and 360^o). The presence of the valleys in airflow speed during spinning process (*Figure 8)* may also explain why the rotor spun yarn evenness is not as good as ring spun yarn.

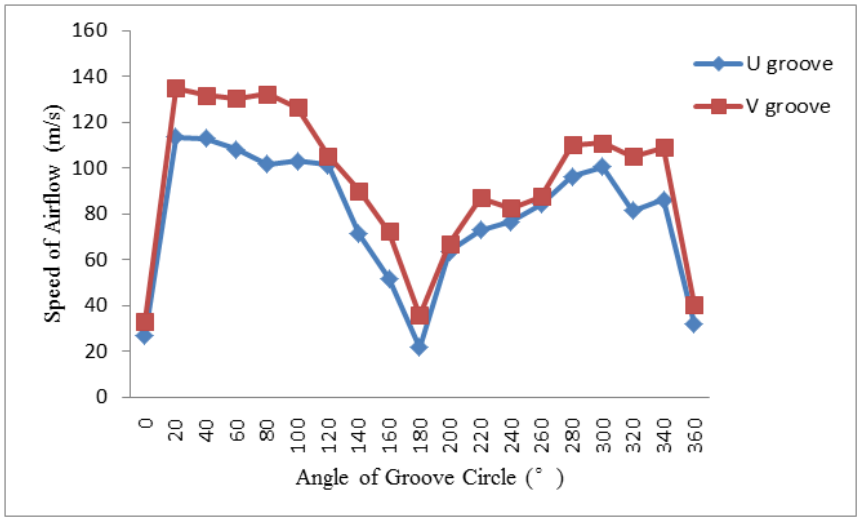

FIGURE 8. Airflow speed at the groove wall (U-type and V-type) from 0 ° to 360°.

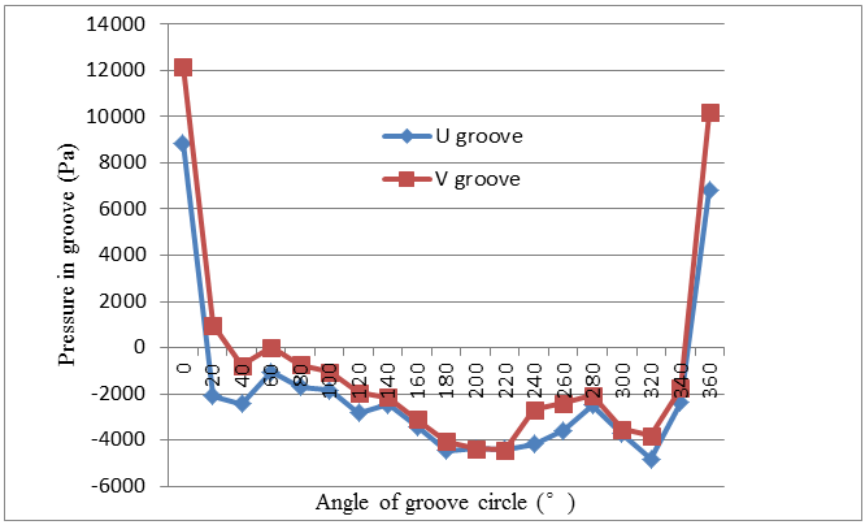

FIGURE 9. Static pressure distribution at the groove wall (U-type and V-type) from 0 ° to 360°.

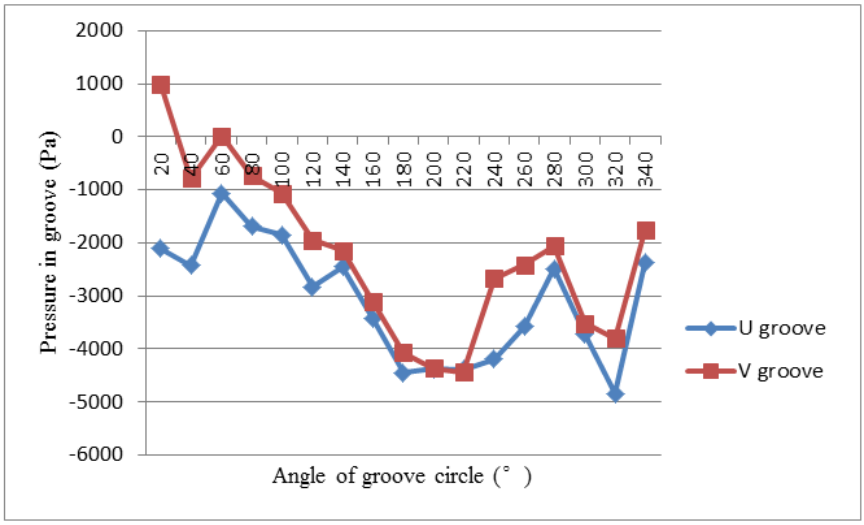

FIGURE 10. Static pressure distribution at the groove wall (U-type and V-type) from 20 ° to 340°.

The static pressures of U and V grooves at the wall showed a similar trend, in the shape of the letter 'W' as shown in *Figure 9.* The plot area is focused between 20 and 340° in *Figure 10* to more clearly indicate the trend in this region. In the case of each groove type, the static pressure at the groove wall reaches a maximum value at 0°, decreases sharply until 40° rotation, decreases slowly to a trough at about 220°, then increases rapidly until about 280° before falling to a second minimum at 320°, finally increasing sharply back to the original value by the time the rotation is complete at 360 degrees.

Figures 8-10 indicate that the airflow speeds produced by the V groove were higher than those produced by the U type. This is because the V type groove has an inverted V bottom, which more easily collects air flow under the action of centrifugal force and packs the fibers more efficiently. This could explain why rotor yarn produced by the V type rotor showed improved evenness, higher breaking strength and more even twist between the inside and outside yarn structure than that produced using the U type rotor. Usually rotor yarn produced using a U type rotor is fluffier and lower in strength with more wrapping fibers [6].

CONCLUSION

Airflow characteristics in rotors with U and V grooves during rotor spinning process were simulated and analyzed. The maximum airflow speeds of the V and U grooves were 134.9 m/s and 113.6 m/s respectively, while the minimum were 21.7 m/s and 35.7 m/s respectively. The valley point of the static pressure of V and U grooves were -4431 Pa and -4834.7 Pa respectively. The data trends in airflow speed and static pressure of different type of groove fit the experimental results- rotor yarn produced using a V type rotor showed improved yarn evenness, higher breaking strength and more even twist than that produced using the U type rotor.

ACKNOWLEDGEMENT

This work was supported by Natural Science Foundation of Jiangsu Province of China No. BK20130148, the National Natural Science Foundation of China No. 51403085, the Fundamental Research Funds for the Central Universities No. JUSRP51631A, and A Project Funded by the Priority Academic Program Development of Jiangsu Higher Education Institutions (PAPD), and the Innovation Fund Project of Cooperation among Industries, Universities & Research Institutes of Jiangsu Province (BY2016022-29).

REFERENCES

[1] Hasani H, Semnani D & Tabatabaei S, Determining the optimum spinning conditions to produce the rotor yarns from cotton wastes, Ind Textila, 61 (6): 259-264 , 2010.

[2] Huh Y, Kim Y R & Oxenham W, Analyzing structural and physical properties of ring, rotor, and friction spun yarns, Tex Res J, 72 (2) : 156-163, 2002.

[3] Chattopadhyay R & Banerjee S, The frictional behaviour of ring-, rotor-, and friction-spun yarn, J Text Inst, 87(1): 59-67, 1996.

[4] Tyagi G K, Goyal A & Dhanda K, Frictional and mechanical properties of mercerized ring- and rotor-spun yarns, Indian J Fiber Text, 29 (3) : 357-361, 2004.

[5] Tyagi G K, Kaushik R C D & Salhotra KR, Indian J Fiber Text, Properties of OE rotor and MJS yarns spun at high spinning speeds, Indian J Fiber Text, 22(1): 8-12, 1997.

[6] Wang S Y & Yu X Y，New Textile Yarns (Donghua University, Shanghai,) Shanghai: Publication of Donghua University, 2006, 93.

[7] Kong L X & Platfoot R A, Tex Res J, Two-dimensional simulation of air flow in tje transfer channel of open-end rotor spinning Machines. Tex Res J, 66(10), 641-650, 1996.

[8] Wang F J. Computational fluid dynamics analysis (Tsinghua University, Beijing), 2004, 7.

[9] Kong L X & Platfoot R A. Fiber transportation in confined channel with recirculations. Comput Struct, 78(1):237-245, 2000.

[10] Launder B E, Spalding D B, Lectures inMathematical Models of Turbulence, London: Academic Press, 55, 1972.

AUTHORS' ADDRESSES

Rui-Hua Yang, PhD
Chao Liu
Yuan Xue
Hongbo Wang
Weidong Gao
Key Laboratory of Eco-textiles
Ministry of Education
Jiangnan University
1800 Lihu Avenue
Wuxi, Jiangsu Province 214122
CHINA